NASA CR-167889
37255-6001-UT-00

INTEGRATED PROPULSION FOR NEAR-EARTH SPACE MISSIONS

VOLUME I: EXECUTIVE SUMMARY

by C.L. Dailey, H.F. Meissinger, R.H. Lovberg, and S. Zafran

TRW Space and Technology Group
Redondo Beach, California 90278

prepared for

NATIONAL AERONAUTICS AND SPACE ADMINISTRATION

NASA Lewis Research Center
Contract NAS 3-22661

ORIGINAL PAGE IS OF POOR QUALITY

1. Report No. CR 167889	2. Government Accession No.	3. Recipient's Catalog No.
4. Title and Subtitle INTEGRATED PROPULSION FOR NEAR-EARTH SPACE MISSIONS, VOLUME I: EXECUTIVE SUMMARY		5. Report Date October 1981
		6. Performing Organization Code
7. Author(s) C. L. Dailey, H. F. Meissinger, R. H. Lovberg, and S. Zafran		8. Performing Organization Report No 37255-6001-UT-00
		10. Work Unit No.
9. Performing Organization Name and Address TRW Defense and Space Systems Group Redondo Beach, California 90278		11. Contract or Grant No. NAS 3-22661
		13. Type of Report and Period Covered Final Report 29 Sep 1980 - 29 Sep 1981
12. Sponsoring Agency Name and Address National Aeronautics and Space Administration Lewis Research Center Cleveland, Ohio 44135		14. Sponsoring Agency Code

15. Supplementary Notes

Project Manager, M. E. Valgora, Systems Analysis Office, NASA - Lewis Research Center

16. Abstract

Tradeoffs between electric propulsion system mass ratio and transfer time from LEO to GEO were conducted parametrically for various thruster efficiency, specific impulse, and other propulsion parameters. A computer model was developed for performing orbit transfer calculations which included the effects of aerodynamic drag, radiation degradation, and occultation. The tradeoff results showed that thruster technology areas for integrated propulsion should be directed towards improving primary thruster efficiency in the range from 1500 to 2500 seconds, and be continued towards reducing specific mass. Comparison of auxiliary propulsion systems showed large total propellant mass savings with integrated electric auxiliary propulsion. Stationkeeping is the most demanding on-orbit propulsion requirement. At area densities above 0.5 m^2/kg, East-West stationkeeping requirements from solar pressure exceed North-South stationkeeping requirements from gravitational forces.

A solar array pointing strategy was developed to minimize the effects of atmospheric drag at low altitude, enabling electric propulsion to initiate orbit transfer at Shuttle's maximum cargo carrying altitude. Gravity gradient torques are used during ascent to sustain the spacecraft roll motion required for optimum solar array illumination. A near optimum cover glass thickness of 6 mils was established for LEO to GEO transfer.

17. Key Words (Suggested by Author(s)) Electric propulsion, Orbit analysis, Large space structures	18. Distribution Statement Unclassified - unlimited

19. Security Classif. (of this report) Unclassified	20. Security Classif. (of this page) Unclassified	21. No. of Pages 25	22. Price*

* For sale by the National Technical Information Service, Springfield, Virginia 22161

NASA-C 168 (Rev 10-75)

NOMENCLATURE

Symbol	
A	Area, m^2
d	Diameter, m
H	Altitude, km
i	Inclination, degrees
M	Mass, kg
p	Duty cycle
α	Specific mass, kg/W
ρ	Specific power, w/m^2 (of drag area)
η	Efficiency
ϕ	Roll angle, degrees
I_{SP}	Specific impulse, sec
ΔV	Velocity increment, m/sec
Subscript	
d	Disposal
E	Electric propulsion (dry)
EP	Electric propulsion (dry)
EPS	Electric propulsion system
f	Final operation
o	Initial
PL	Payload
T	Total propulsion (primary plus auxiliary)

PRECEDING PAGE BLANK NOT FILMED

SUMMARY

Previous studies established categories for primary and auxiliary electric propulsion in near-earth missions (References 1 and 2, respectively). In addition, Reference 3 characterized missions to be deployed from the Space Transportation System in low earth orbit. This study extended previous results to encompass integrated electric propulsion systems. The objectives of this effort were to establish the nature and characteristics of electric propulsion systems (1) that can provide the propulsion required for all phases of the LEO to GEO mission, starting with the spacecraft assembled in low earth orbit, and continuing through spacecraft disposal after conclusion of on-orbit operations, and (2) whose characteristics have minimum sensitivity to changes in mission requirements, thereby assuring as wide an applicability of the systems as possible.

The propulsion functions studied are listed in Table 1. The analytical approach employed is outlined on Table 2. The gravitational equation was solved for direct determination of orbit transfer time as a function of payload mass ratio. Transfer time computations included occultation, aerodynamic drag, and radiation environment effects. A feathered array strategy was developed for low altitude flight, where the solar array was aligned edge-on to the flight direction to provide minimum drag, and the spacecraft was rolled for optimum array illumination. Above the atmospheric drag region (>400 km altitude), the array was rotated about its axis and the spacecraft was rolled to track the sun angle. Gravity gradient torques were found to assist in sustaining the periodic roll motion. Plane change was initiated above 10,000 km to minimize radiation degradation.

The rocket equation was used for analyzing propulsion functions other than orbit boosting.

Primary thruster efficiency was varied parametrically. Three efficiency functions, as shown in Figure 1, were defined for study. The Case I and Case II efficiency functions are lower and upper bounds respectively of present-day high performance ion thrusters. The Case III function is an estimated upper limit that may be approached with further development. The specific impulse for auxiliary propulsion was set at its state-of-the-art value of 3000 seconds for all calculations.

Tradeoff calculations were made to determine the optimum solar cell cover thickness for LEO to GEO orbit transfer. Specific mass and thruster efficiency were varied from their highest to lowest values for these calculations. The results showed that 6-mil cover thickness, on both sides of the solar array, yielded very close to the minimum thrust times for all combinations of efficiency and specific mass, and a residual power factor on orbit that increased only slightly with thicker covers. Accordingly, 6-mil covers were used for subsequent analysis.

Conservative calculations of solar array drag effects based on total array area, i.e., with the array perpendicular to the flight direction,

Table 1. Propulsion Fu·ctions Investigated

- **ORBIT BOOSTING**
- **INCLINATION CHANGE**
- **ATTITUDE CONTROL**
- **STATIONKEEPING**
- **RELOCATION**
- **DISPOSAL**
- **POWER SHARING ON-ORBIT**

Table 2. Analytical Approach

- **ORBIT BOOSTING**
  - **SOLVED GRAVITATIONAL EQUATION**
  - **ADDED OCCULTATION**
  - **ADDED AERODYNAMIC DRAG**
  - **ADDED RADIATION DEGRADATION**
  - **DEVELOPED OPTIMUM ARRAY ILLUMINATION STRATEGY**
- **ALL OTHER FUNCTIONS**
  - **IMPLEMENTED ROCKET EQUATION**
- **I_{sp} FOR AUXILIARY PROPULSION SET AT 3000 SEC**
- **PLANE CHANGE INITIATED ABOVE RADIATION BELT**

ORIGINAL PAGE IS
OF POOR QUALITY

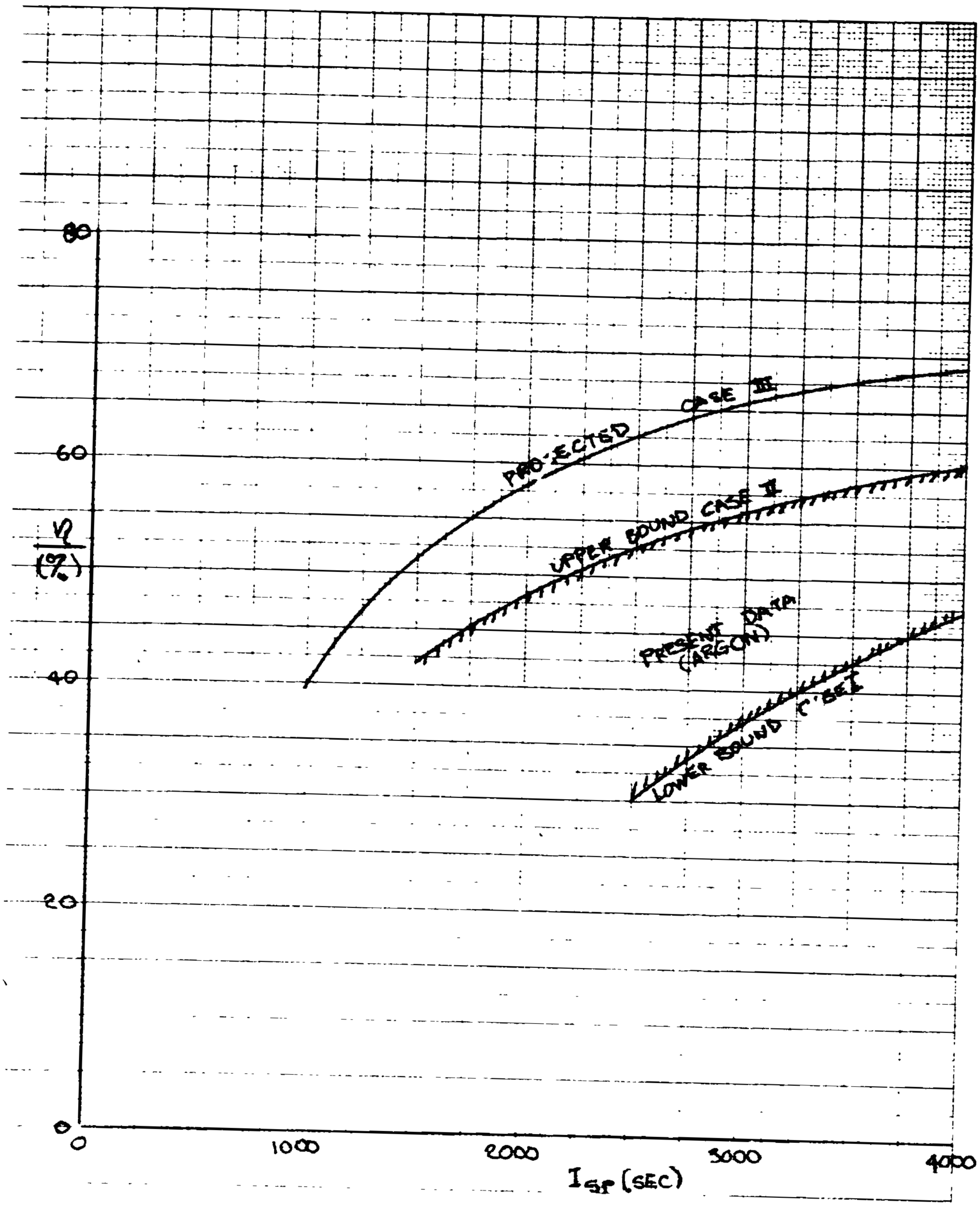

Figure 1. Thruster Efficiency Functions

impose an unrealistic limitation on minimum useful altitude for solar power. The limit occurs well above the Shuttle parking orbit for maximum payload, (about 250 km). This apparent limitation is readily removed by a feathered array strategy in which the array is oriented parallel to the flight direction and the spacecraft is rolled to the angle for maximum illumination. This reduces the available power but the drag area is reduced considerably more than the power with the result that the power per unit drag area β_E is increased by about a decade. Sustained flight is then possible at altitudes considerably lower than the Shuttle orbit, and electrically propelled spacecraft deployment directly from Shuttle becomes practical.

The minimum altitude relations for nuclear and solar-electric spacecraft are plotted in Figure 2. The electric propulsion dry mass, M_{EP}, included thrusters, power source, power conditioning, gimbals, propellant storage and distribution, structure, and thermal control for propulsion equipment. The payload mass, M_{PL}, contained the remaining (dry) mass deployed from the Shuttle Orbiter. With a nuclear power source, electric propulsion was estimated to have a specific mass α_E = 0.033 while for solar power α_E ranged from 0.012 to 0.036 (kg/W).

The most important conclusion to be drawn from Figure 2 is that sustained flight with electric propulsion is practical down to 150 km, i.e., 100 km below the Shuttle parking orbit for maximum payload delivery. In this high drag region, the feathered solar array performs as well as the nuclear source. Thus, solar electric propulsion can be used directly to augment Space Transportation System capability without relying on intermediate chemical propulsion stages. Solar electric orbit transfer vehicles, servicing vehicles, or on-board propulsion systems may be deployed directly from the Shuttle Orbiter.

The effect of primary thruster efficiency and specific impulse on orbit transfer time was analyzed for different values of electric propulsion system mass ratio. The mission parameter set is shown in Table 3. M_{EPS} is the total electric propulsion system mass, including primary and auxiliary propellant, needed to perform the LEO to GEO mission. This mission starts at 250 km Shuttle parking altitude at 28.5 degrees inclination, includes orbit transfer to GEO, up to 10 years on-orbit operations, and disposal afterwards. The on-orbit ΔV requirements listed on Table 3 provide for ±0.1 stationkeeping, attitude control, and disposal of a spacecraft size consistent with a single Shuttle launch.

The tradeoff results of transfer times for various electric propulsion system to payload mass ratios are shown in Figures 3 through 7. The figures exhibit an optimum I_{SP}, independent of η, that produces the shortest trip time for a given efficiency. Also plotted on these curves is the Case II efficiency relation, which shows the characteristic droop toward lower I_{SP}. The net effect of this droop, as shown in Table 4, is that minimum trip time occurs at higher I_{SP} than the optimum value.

From a system point of view, it is more economical to operate at an I_{SP} slightly lower than the minimum transfer time value in order to reduce the more expensive electric propulsion mass while increasing the less expensive propellant mass. A typical mass breakdown is shown in Figure 8 for 33% payload fraction. Payload fraction is the ratio of payload mass

ORIGINAL PAGE IS
OF POOR QUALITY

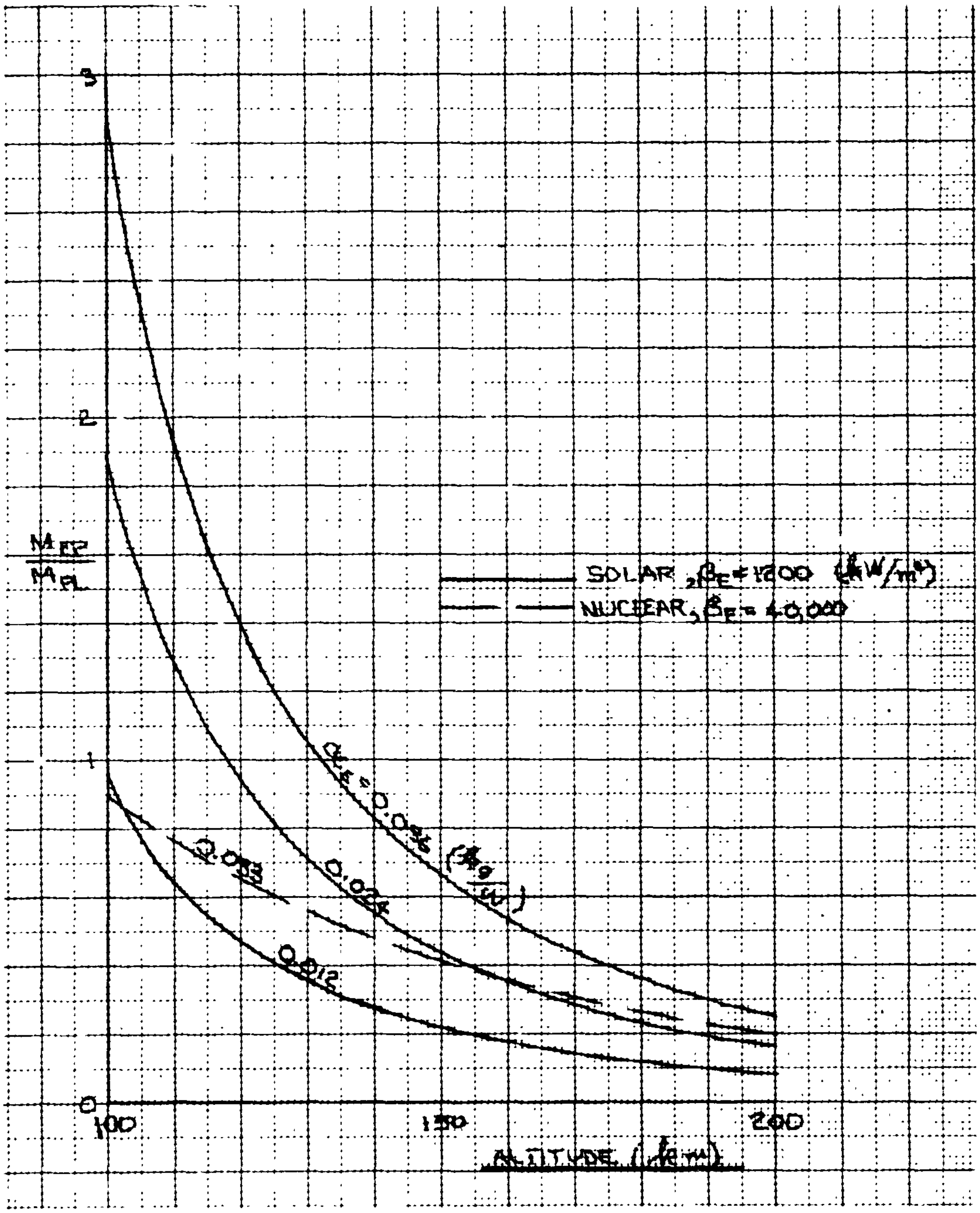

Figure 2. Comparison of Minimum Altitude for Feathered Solar and Nuclear Power

ORIGINAL PAGE IS
OF POOR QUALITY

Table 3. Mission Parameter Set

Mission Set No.	$\left(\frac{M_{EPS}}{M_{PL}}\right)_T$	Lifetime on Orbit (years)	ΔV on Orbit $\left(\frac{m}{sec}\right)$
1	1.0	10	1731
2	2.0	10	1731
3	3.0	10	1731
4	4.0	10	1731
5	2.0	5	949

Initial altitude, H_0 =250 km
Final operation altitude, H_f = 35786 km
Initial inclination, i_o = 28.5°
Final operation inclination, i_f = 0° (equatorial orbit)
Disposal altitude, H_d = 40786 km

$\left(\frac{M_{EPS}}{M_{PL}}\right)_T$ represents the ratio of the total propulsion mass (primary thruster system dry, primary propellant and auxiliary propulsion required for stationkeeping and disposal) to the payload mass.

Table 4. Comparison of Optimum I_{SP} and I_{SP} For Minimum Transfer Time - Case II Efficiency

$\left(\frac{M_{EPS}}{M_{PL}}\right)_T$	Optimum I_{SP} (sec)	I_{SP} For Minimum Transfer Time (sec)
1	2600	3100
2	1750	2300
3	1550	2000
4	1400	1800

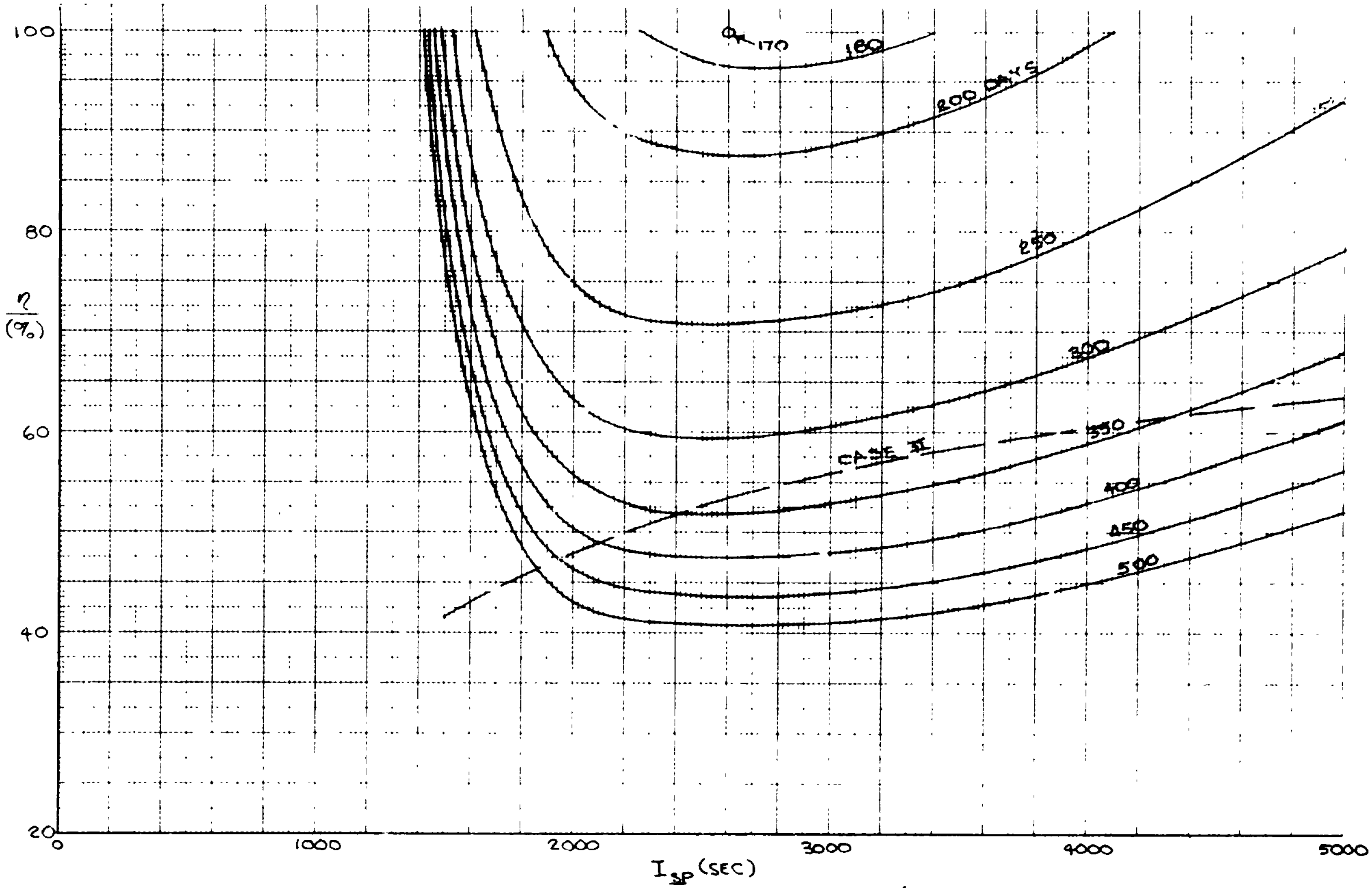

Figure 3. Effect of η & I_{SP} on Transfer Time for $\left(\frac{M_{EPS}}{M_{PL}}\right)_T = 1.0$

$$\left(\alpha = 0.024\ \frac{kg}{W},\ \beta = 150\ \frac{W}{m^2},\ \frac{M_{PL}}{A_{PL}} = 100\ \frac{kg}{m^2},\ 10\ \text{years}\right)$$

ORIGINAL PAGE IS
OF POOR QUALITY

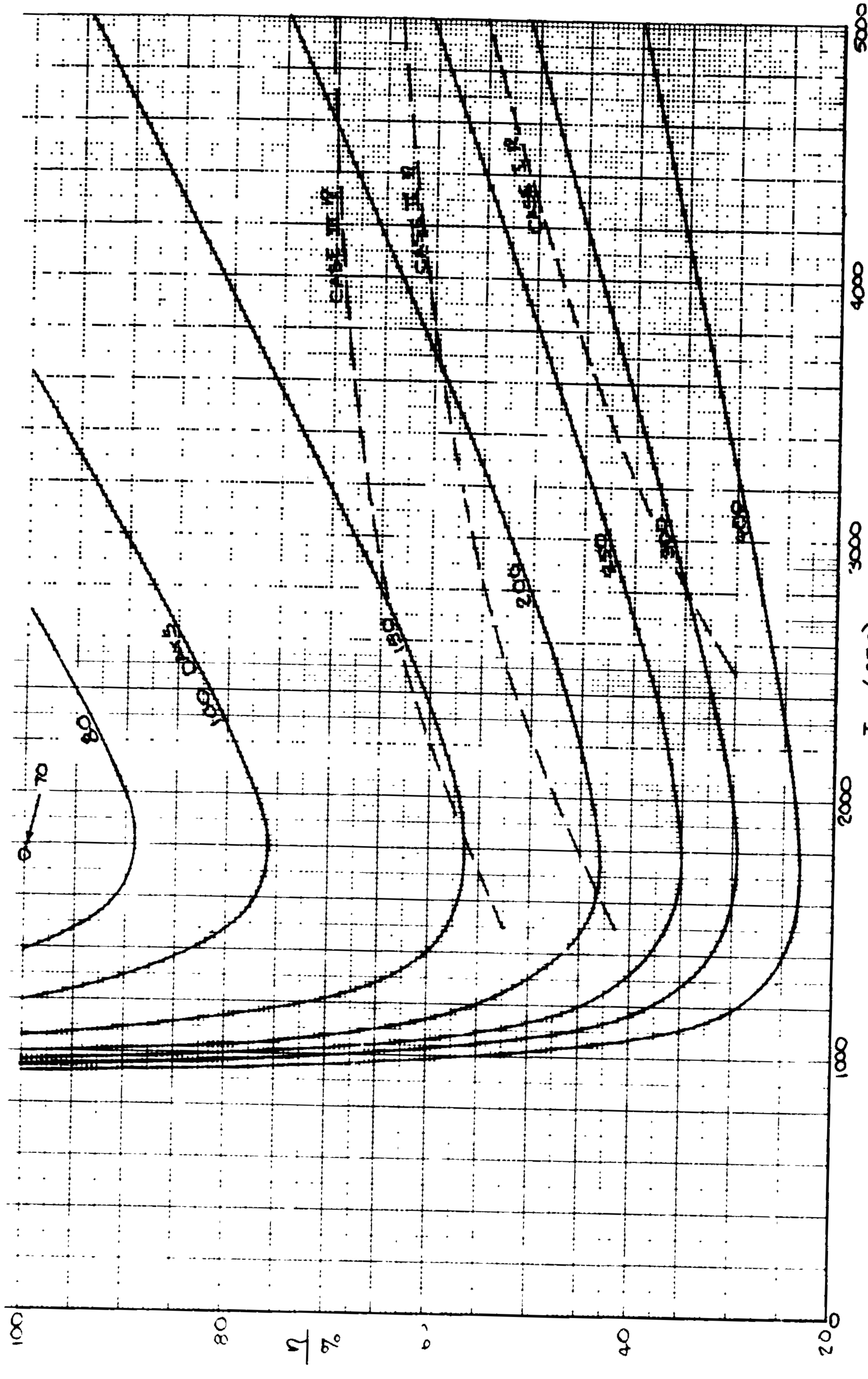

Figure 4. Effect of η & I_{SP} on Transfer Time for $\left(\frac{M_{EPS}}{M_{PL}}\right)_T = 2.0$

$\left(\alpha = 0.024\ \frac{kg}{W},\ \beta = 150\ \frac{W}{m^2},\ \frac{M_{PL}}{A_{PL}} = 100\ \frac{kg}{m^2},\ 10\ \text{years}\right)$

ORIGINAL PAGE IS
OF POOR QUALITY

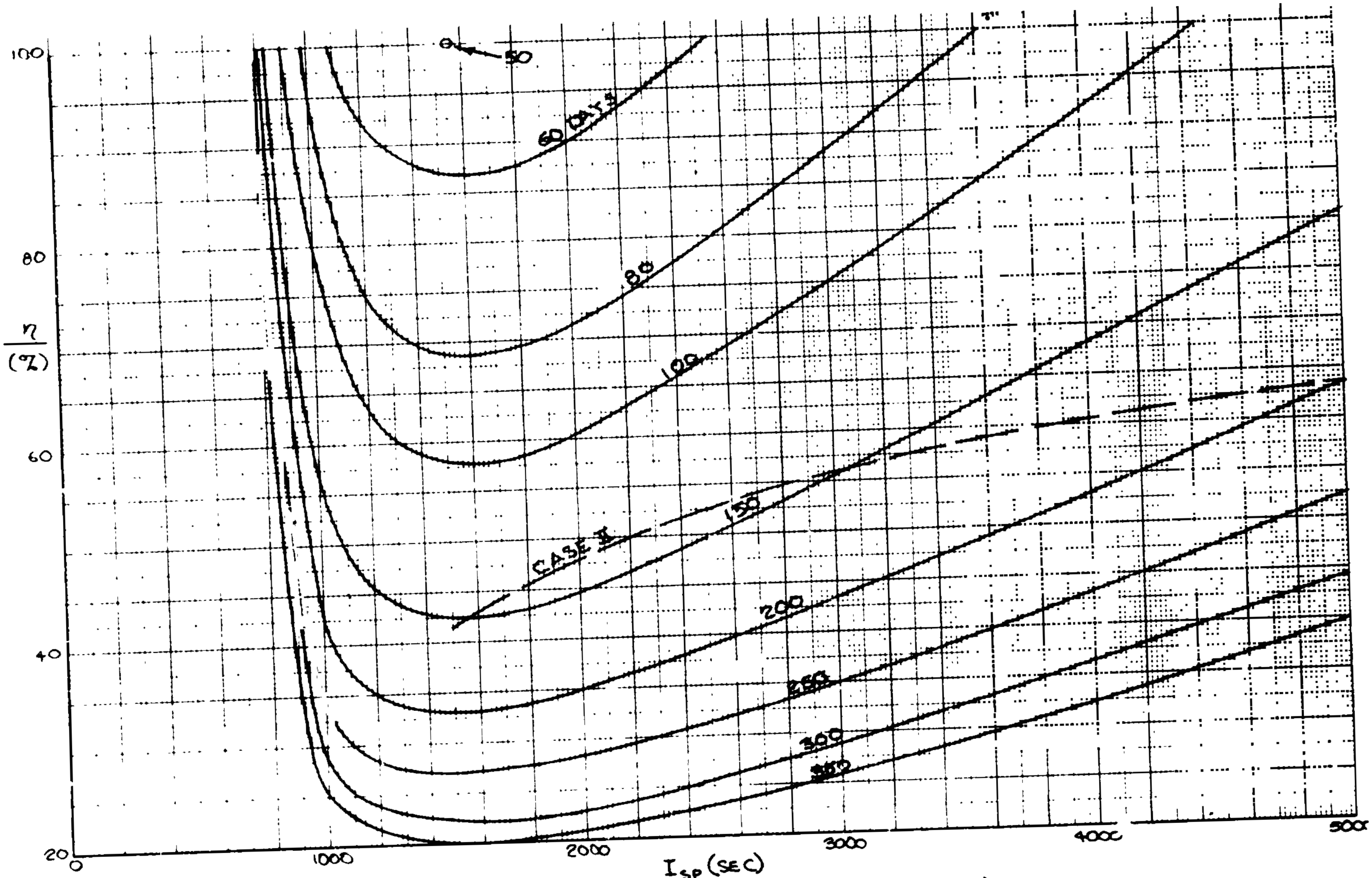

Figure 5. Effect of η & I_{sp} on Transfer Time for $\left(\frac{M_{EPS}}{M_{PL}}\right)_T = 3.0$

$\left(\alpha = 0.024\ \frac{kg}{W},\ \beta\ \ \frac{W}{\eta^2},\ \frac{M_{PL}}{A_{PL}} = 100\ \frac{kg}{m^2},\ 10\ \text{years}\right)$

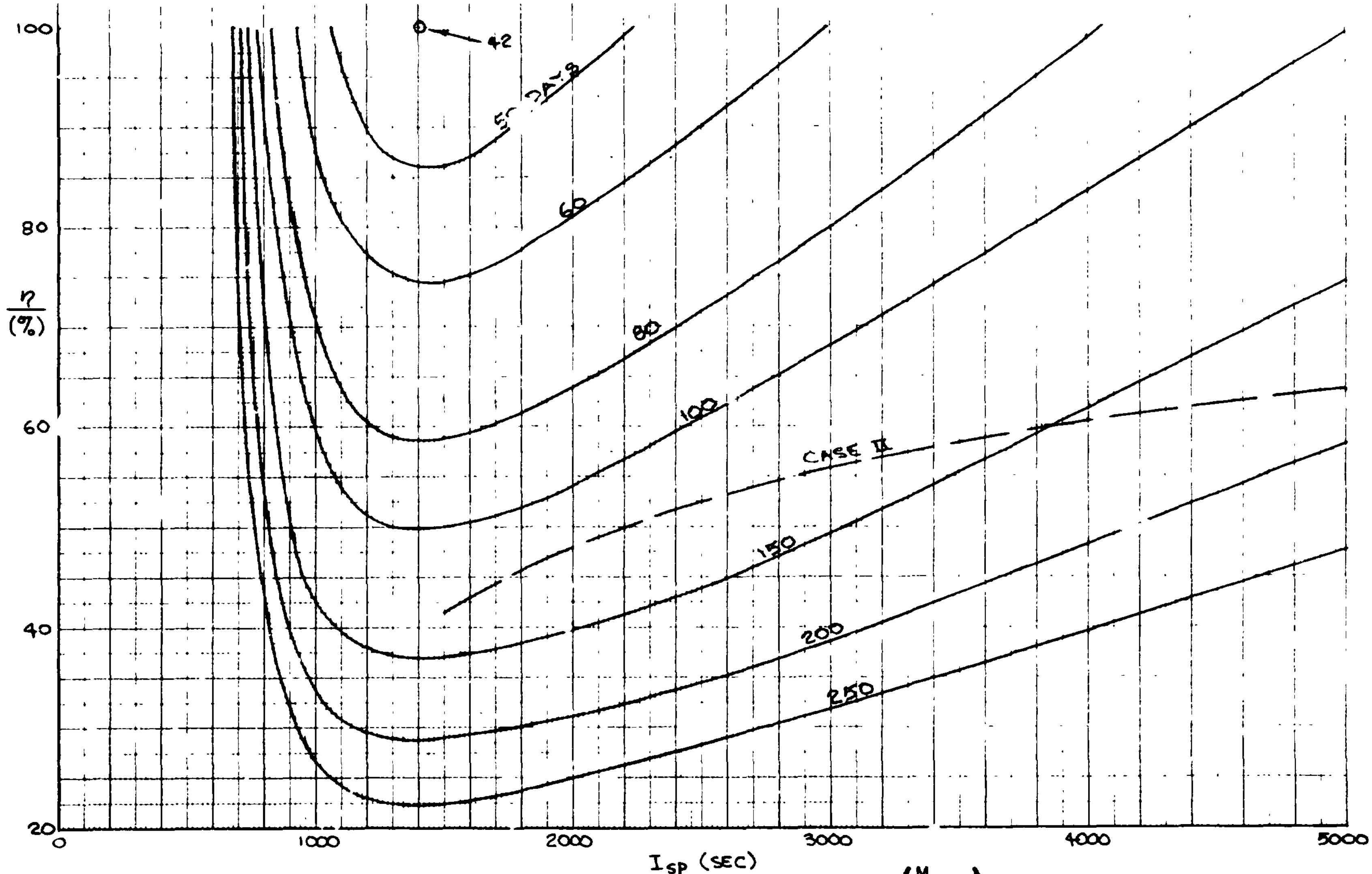

Figure 6. Effect of η & I_{SP} on Transfer Time for $\left(\frac{M_{EPS}}{M_{PL}}\right)_T = 4.0$

$\left(\alpha = 0.024 \frac{kg}{W}, = 150 \frac{W}{m^2}, \frac{M_{PL}}{A_{PL}} = 100 \frac{kg}{m^2}, 10 \text{ years}\right)$

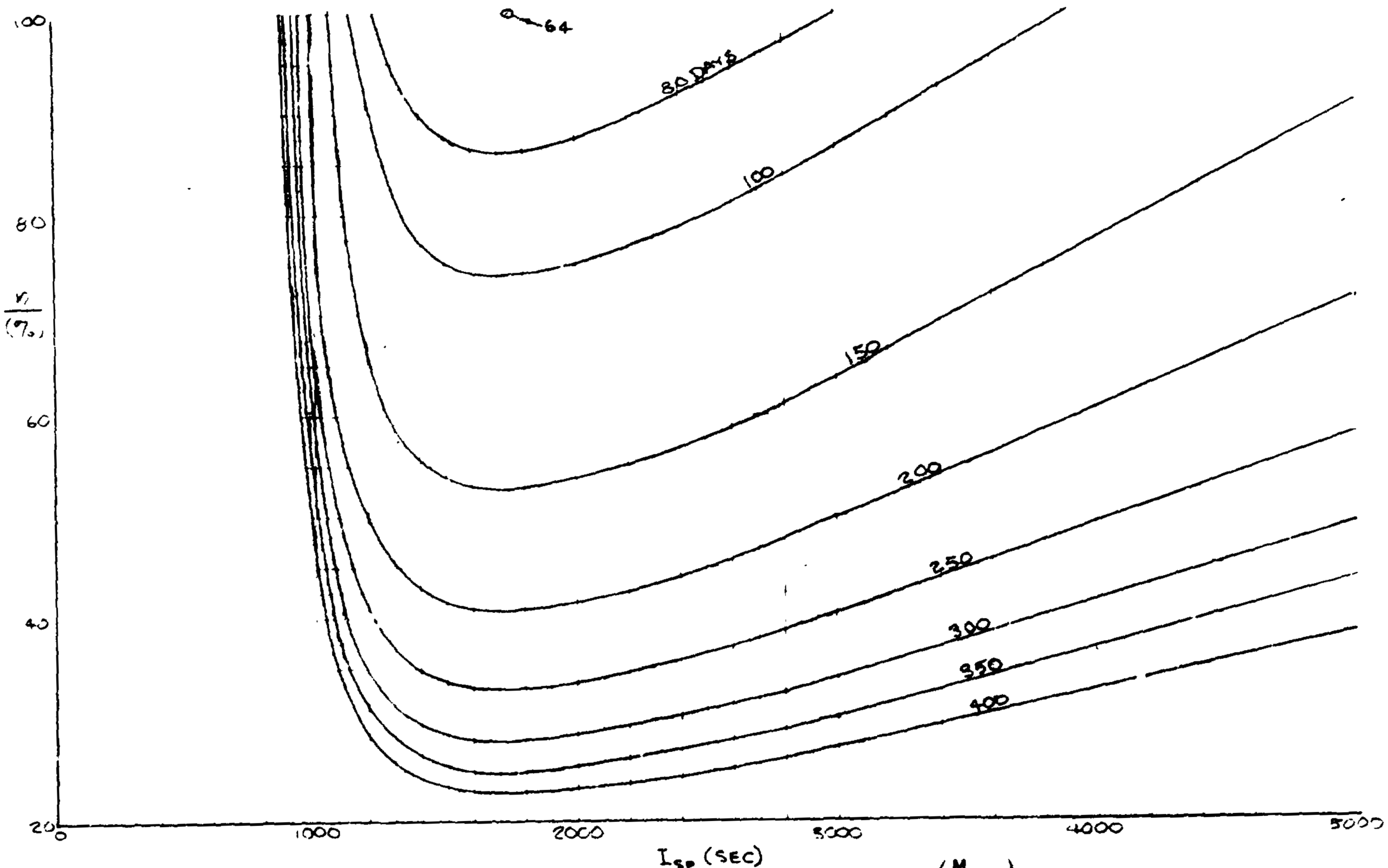

Figure 7. Effect of η and I_{SP} on Transfer Time for $\left(\frac{M_{EPS}}{M_{PL}}\right)_T = 2.0$

$\left(\alpha = 0.024\ \frac{kg}{W},\ \beta = 150\ \frac{W}{m^2},\ \frac{M_{PL}}{A_{PL}} = 100\ \frac{kg}{m^2},\ 5\ \text{years}\right)$

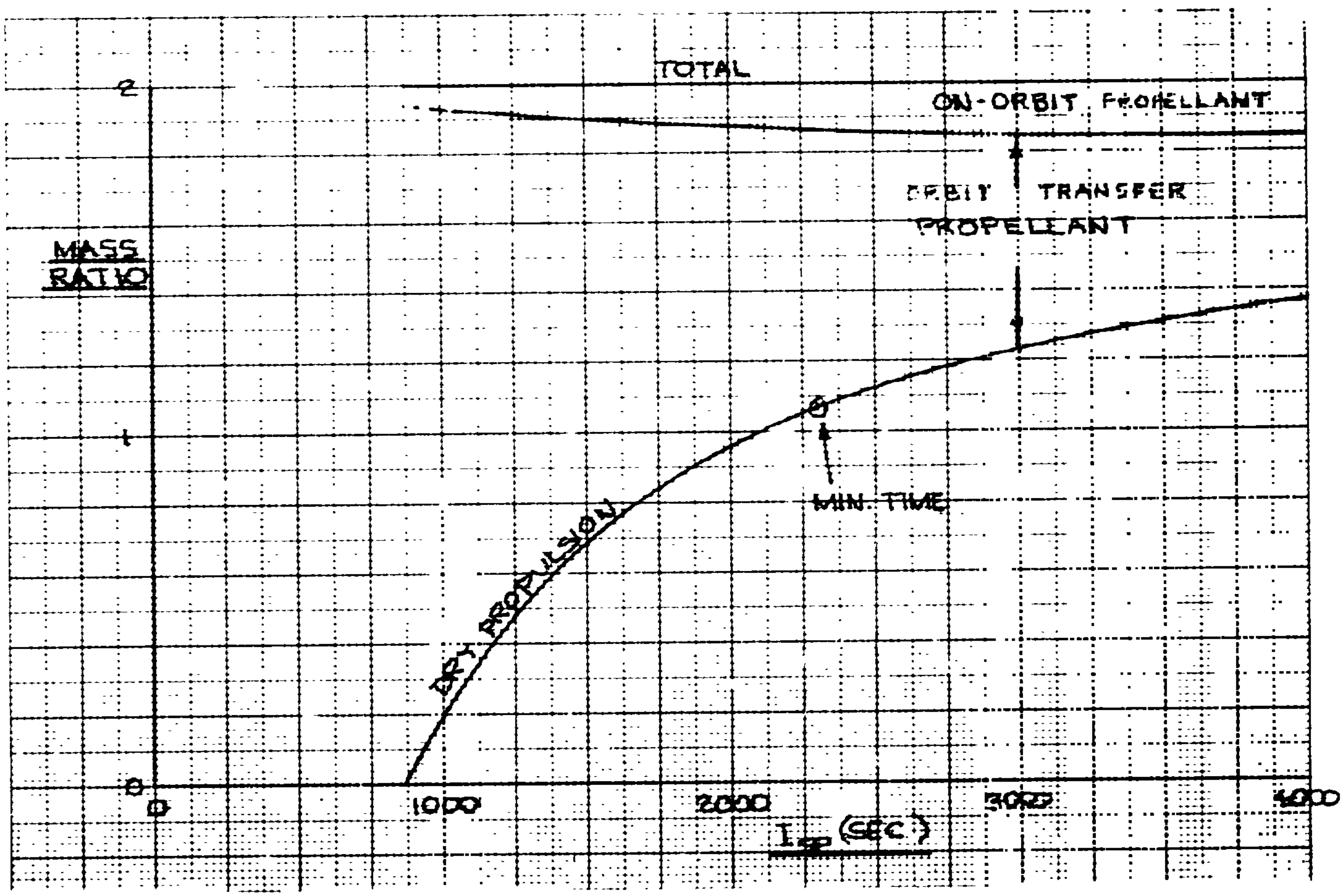

Figure 8. Propulsion Mass Breakdown for 33% Payload Fraction (Case II η, α = 0.024 kg/W, 10 Years)

to total deployed spacecraft mass. It is related to the total electric propulsion system mass ratio as follows:

$$\text{Payload Fraction} = \frac{1}{\left(\frac{M_{EPS}}{M_{PL}}\right)_T + 1}$$

The reduction of on-orbit lifetime requirements from 10 to 5 years has a small effect on transfer time as can be seen in Figure 9.

The two thruster parameters that have the greatest impact on transfer time are thruster efficiency and the electric propulsion specific mass parameter α. Figure 10 is a cross-plot of Figures 3 through 6 showing transfer time as a function of thruster efficiency at the optimum I_{SP} for the four different values of the total electric propulsion mass ratio. The corresponding optimum I_{SP} values are also shown. For the case of mass ratio equal to 2.0 at 50% efficiency, for example, the slope corresponds to a 3.7-day reduction in transfer time for a 1% improvement in thruster efficiency.

Figure 11 shows that transfer time varies essentially linearly with α. For a total electric propulsion mass ratio of 2.0 and a thruster efficiency of 45% at 1750 seconds I_{SP}, the slope at α = 0.024 kg/W indicates a transfer time reduction of 20 days for a 10% reduction in α.

For the LEO to GEO transfer mission, thruster technology effort should be focused on increasing efficiency at moderate I_{SP} (1500 to 2500 seconds) and reducing the specific mass as much as possible. Any thruster capable of achieving both of these objectives simultaneously would be very attractive for this mission.

Figure 12 shows the power remaining after orbit transfer as a function of total EPS mass ratio, assuming the climb is conducted at optimum I_{SP} and Case II efficiency. In the mass ratio range of 2 to 4, the residual power ranges from 55 to 59% of the beginning of life value. At a mass ratio of 1.0, it is 50% of the initial value. The on-orbit power degradation is small. Table 5 compares the integrated fluence over a 10-year mission with that accumulated during orbit transfer and with the total fluence per 11-year solar cycle. The total on-orbit increment is about 2% of the orbit transfer value.

Integrated propulsion analysis was performed to identify potential advantages of using electric propulsion not only for orbit raising to geosynchronous orbit but also for additional (auxiliary) functions that will be required during the ascent and orbital phases of the mission. These functions can be accomplished by using the electric propulsion system (EPS) as an integrated part of the space vehicle rather than as a separate orbit transfer vehicle only.

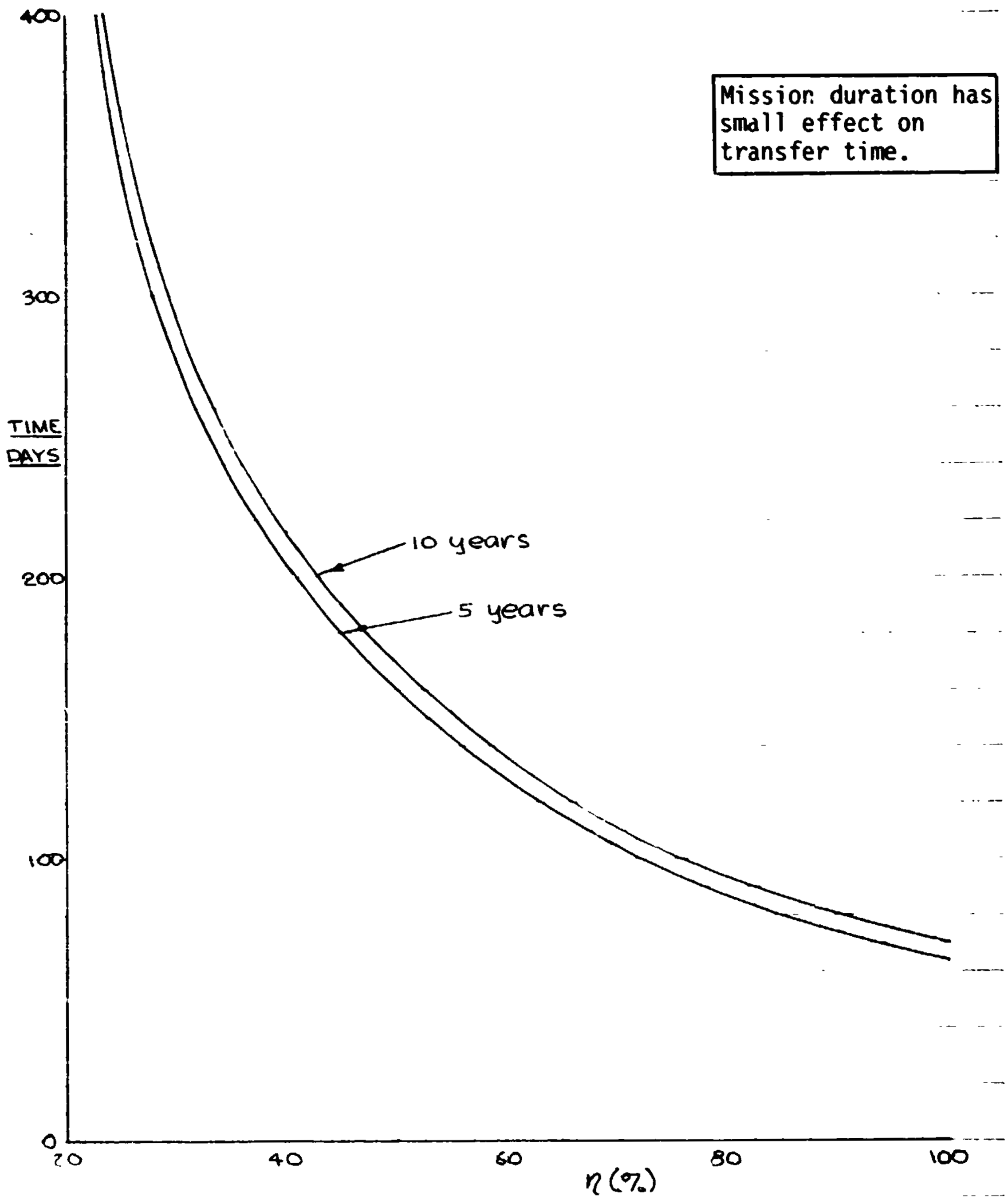

Figure 9. Comparison of Transfer Times for 5 and 10 Year Missions

$$\left(\alpha = 0.024\ \frac{kg}{W},\ \beta = 150\ \frac{W}{m^2},\ \frac{M_{PL}}{A_{PL}} = 100\ \frac{kg}{m^2},\ \text{Orbit Transfer } I_{SP} = 1750\text{ sec},\ \text{Auxiliary } I_{SP} = 3000\text{ sec},\ \left(\frac{M_{EPS}}{M_{PL}}\right)_T = 2.0\right)$$

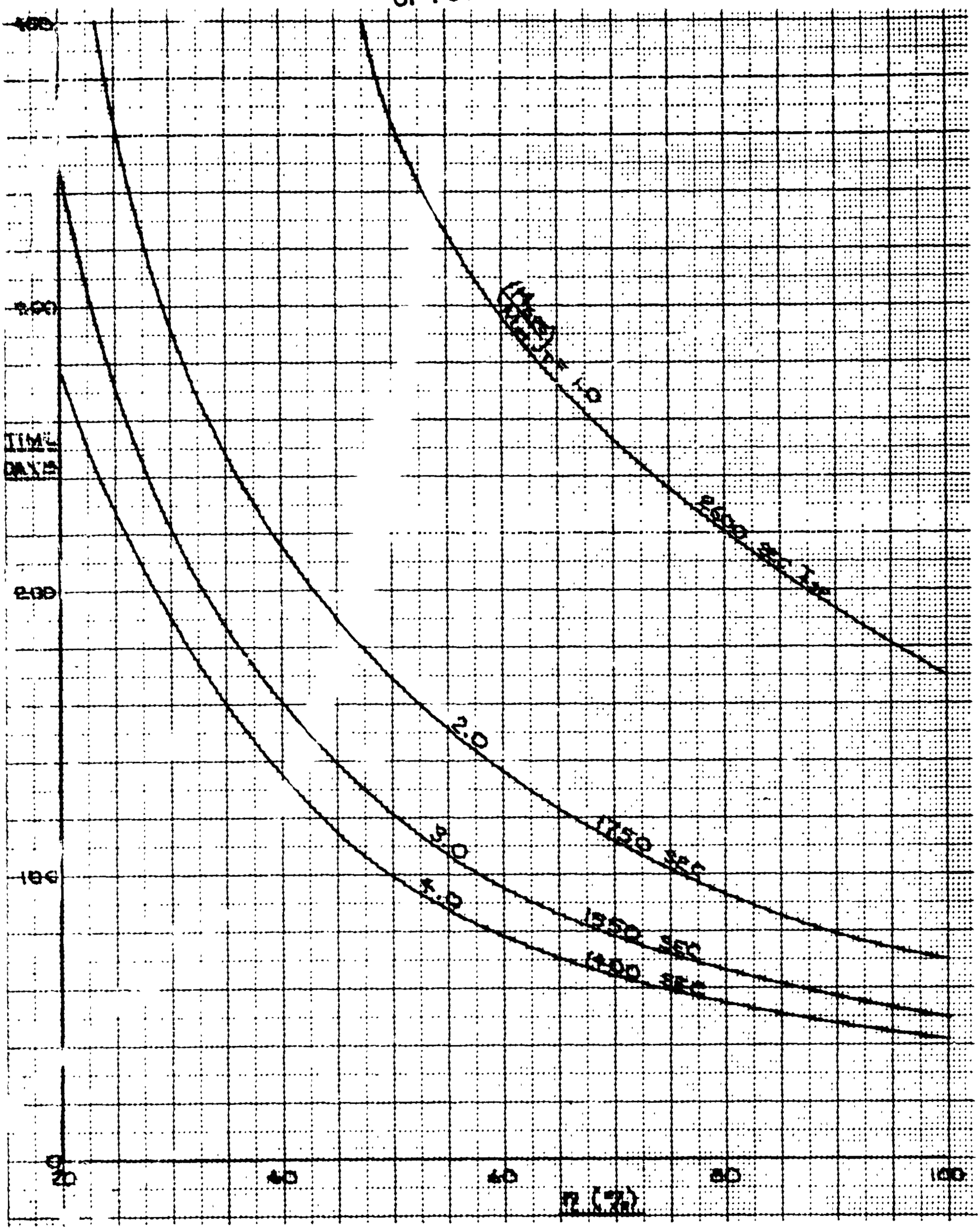

Figure 10. Effect of η on Transfer Time at Optimum I_{SP}

$$\left(\alpha = 0.024\ \frac{kg}{W},\quad \beta = 150\ \frac{W}{m^2},\ \frac{M_{PL}}{A_{PL}} = 100\ \frac{kg}{m^2},\ 10\ \text{years}\right)$$

ORIGINAL PAGE IS
OF POOR QUALITY

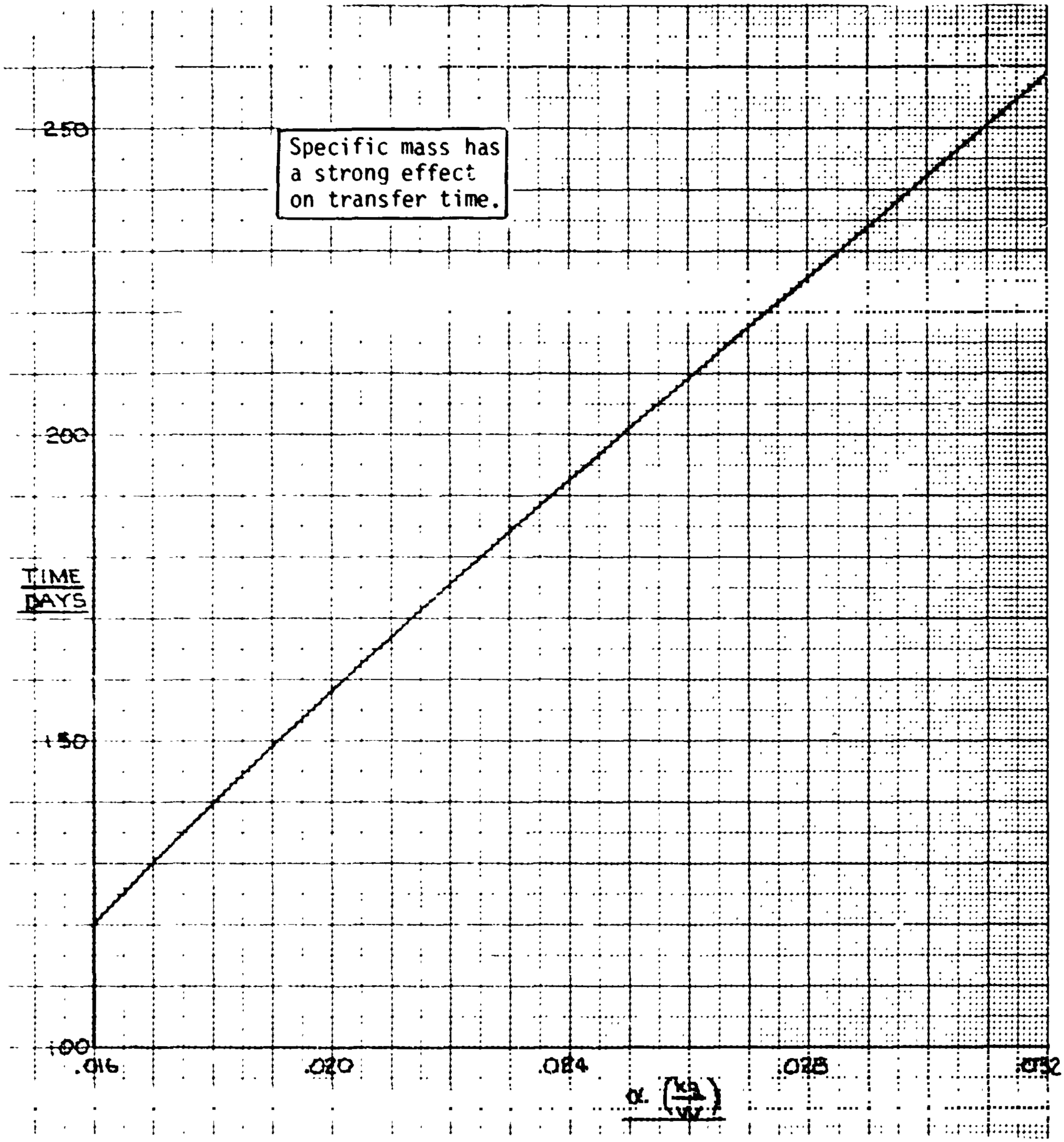

Figure 11. Effect of Specific Mass on Transfer Time for Case II η = 45% at 1750 sec

$$\left[\beta = 150\ \frac{W}{m^2}\ ,\ \ \frac{M_{PL}}{A_{PI}} = 100\ \frac{kg}{m^2}\ ,\ \left(\frac{M_{EPS}}{M_{PL}}\right)_T = 2.0\right]$$

ORIGINAL PAGE IS
OF POOR QUALITY

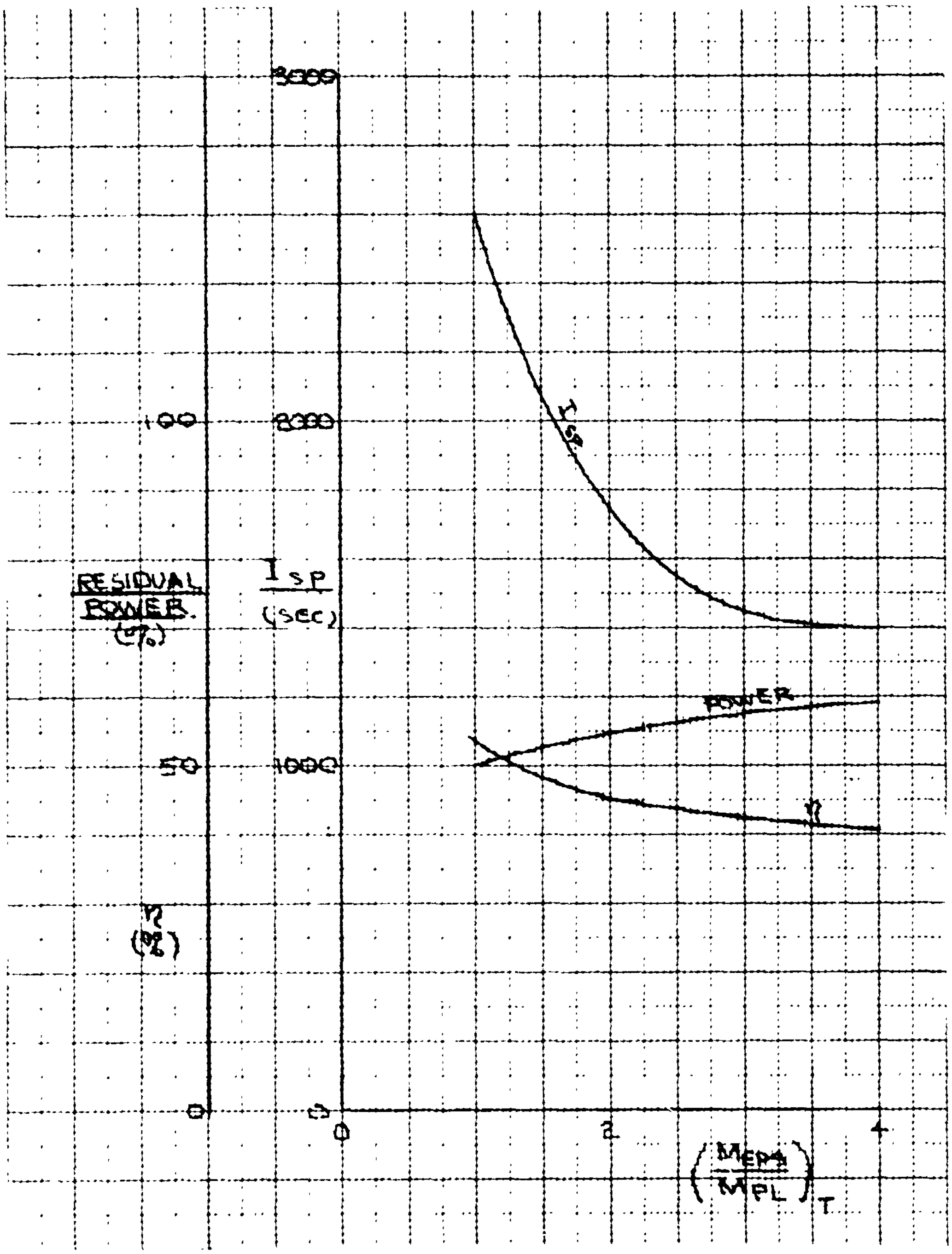

Figure 12. Residual On-Orbit Power for Optimum I_{SP} Transfer and Case II Efficiency

(α = 0.024 kg/W, β = 150 W/m^2, M_{PL}/A_{PL} = 100 kg/m^2, 10 years)

ORIGINAL PAGE IS
OF POOR QUALITY

Table 5. Comparison of Orbit Transfer and On-Orbit Fluence Levels $\left(\frac{\text{meV electrons}}{\text{cm}^2}\right)$

$\left(\frac{M_{EPS}}{M_{PL}}\right)_T$	Orbit Transfer	10-year Increment	Solar Flare	Total	Residual Power (%)
1.0	3×10^{16}	1.8×10^{14}	3×10^{14}	3.05×10^{16}	50
2.0	2.7×10^{16}	1.8×10^{14}	3×10^{14}	2.55×10^{16}	55
3.0	1.55×10^{16}	1.8×10^{14}	3×10^{14}	1.60×10^{16}	58
4.0	1.50×10^{16}	1.8×10^{14}	3×10^{14}	1.55×10^{16}	59

This study made use of results obtained from previous and concurrent studies of auxiliary electric propulsion systems on large space structures performed by Boeing Aerospace Company (Reference 2). A wide range of spacecraft configuration categories, masses and dimensions are covered in the Boeing report, with emphasis on large structures that require multiple Shuttle launches and assembly in orbit. For the present analysis, data applicable to a class of intermediate-sized vehicles with nearer-term mission application prospects were selected.

The data used pertain to a spacecraft category termed "modular antenna structure" (see Figure 13) with a mass ranging from 2000 to 27,000 kg. Spacecraft characteristics in the lower mass range are compatible with a single Shuttle launch. The one-axis gimballed solar arrays provide primary propulsion power of several hundred kilowatts. This implies array sizes of several thousand square meters with tip-to-tip dimensions of hundreds of meters. Data for this spacecraft class are presented in the Boeing report with antenna size as scaling parameter (d ranging from 15 to 200 m). Corresponding solar array dimensions range to 70 m panel length.

The most significant on-orbit propulsion requirements are for stationkeeping. For large spacecraft structures with high area-to-mass ratios, A/M, such as those considered in this study, the annual E-W stationkeeping ΔV expenditures required to compensate for the effects of earth's triaxiality are negligible by comparison to solar pressure effects.

Figure 14 presents annual east-west and north-south stationkeeping requirements as a function of spacecraft area-to-mass ratio with the duty cycle p as a parameter. The value p = 0 corresponds to impulsive thrusting, p = 1.0 to continuous thrusting over the entire orbit during days

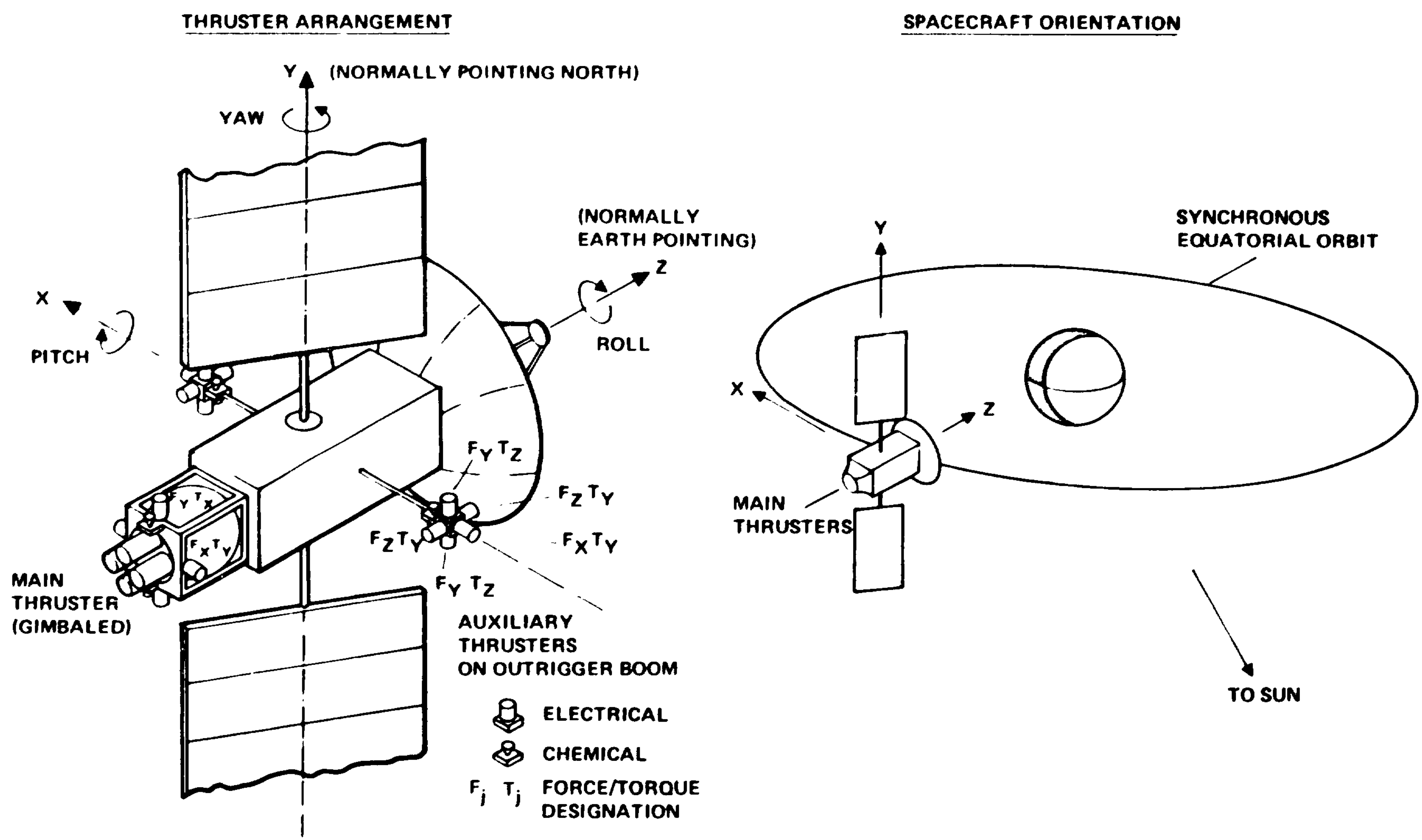

Figure 13. Modular Antenna Spacecraft Configuration

ORIGINAL PAGE IS OF POOR QUALITY

ORIGINAL PAGE IS
OF POOR QUALITY

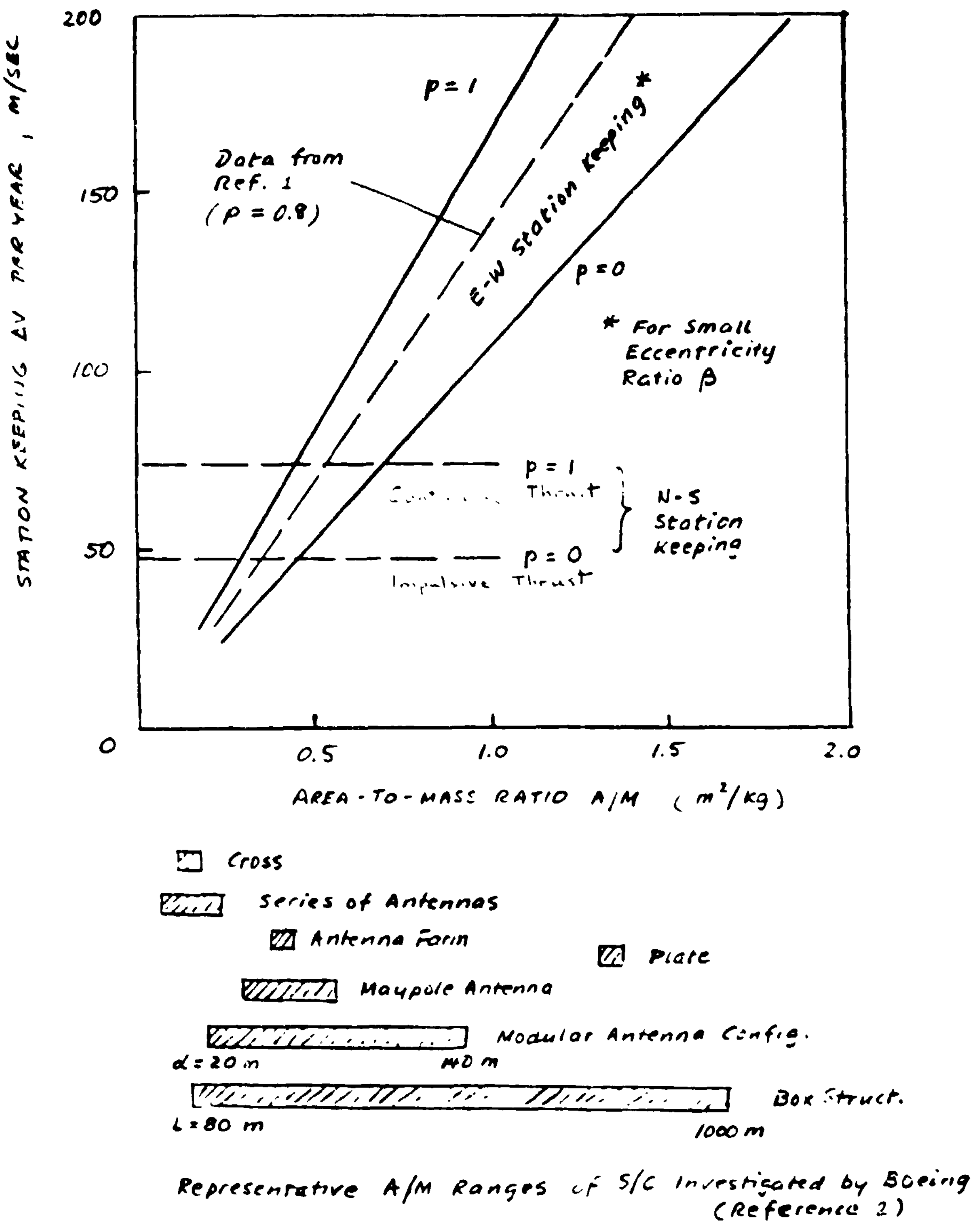

Figure 14. Stationkeeping ΔV Requirements vs A/M Ratio and Representative A/M Ranges for Various S/C Classes

when stationkeeping maneuvers are being performed. In low thrust operation, both E-W and N-S stationkeeping ΔV requirements increase with the length of the duty cycle. The penalty factor is $\pi/2 = 1.571$ for $p = 1.0$ relative to impulsive thrust maneuvers (where $p = 0$). Figure 14 shows that the ΔV required for E-W stationkeeping exceeds the N-S stationkeeping ΔV if the A/M ratio is greater than 0.45 m^2/kg, assuming the same duty cycle is used in either case. Typical ranges of A/M values for seven classes of large spacecraft investigated in the Boeing study are indicated below in the abscissa. For the modular antenna class of spacecraft assumed as typical in the present study, the E-W stationkeeping requirements range from 20 to 100 m/sec per year as A/M varies between 0.17 and 0.90 m^2/kg, i.e., for antenna diameters ranging from 20 to 140 m. In this case the E-W stationkeeping requirements exceed those for N-S stationkeeping if $d > 60$ m.

Comparison was made between a chemical auxiliary propulsion system (APS) operating at 300 seconds I_{sp}, and an electric APS at 3000 seconds I_{sp}. Repositioning and disposal in the electric case were performed by the main thrusters (of the integrated EPS) at 1500 seconds I_{sp}. The mass characteristics are shown graphically in Figure 15 for comparison.

Note that for the 60 m antenna spacecraft, the use of electric APS saves over 7000 kg of total launched weight. At the Shuttle cargo limit of 29,500 kg, electric APS affords about a 50% increase in reference spacecraft mass.

During the ascent phase of the mission, gravity gradient torques can be employed to assist in orienting the spacecraft for optimum array illumination. The spacecraft attitude maneuvers required are summarized in Table 6. In the atmospheric drag region, the solar arrays are feathered for minimum drag. The spacecraft is either maintained fixed at ϕ (roll angle) = 90 degrees or rolled from ±38 to ±75 degrees with sun angle variation. Gravity gradient is useful in providing restoring torques towards $\phi = 0$. The maximum gravity gradient torques are near $\phi = \pm 45$ degrees, which are consistent with maneuver requirements. The best utilization of gravity gradient occurs when the period of roll motion is close to that of the orbital period. At low to intermediate altitudes, above the drag region, the solar arrays are rotated about their axis, and the roll motion is the same as described above. At intermediate to high altitudes, when combined orbit boosting and plane change are implemented, the roll motion is similar to that described above, but is modified to accommodate additional yaw motion for optimum solar array illumination.

The gravity gradient assist is most useful at low altitudes, where torque requirements are greatest, for reducing the size of inertial momentum storage devices in the attitude control system. Since the roll motion is driven primarily by gravity gradient, rather than by spacecraft attitude control moment gyroscopes or reaction control, solar array deformations are also reduced. If possible, spacecraft mass distribution should be chosen to permit gravity gradient operation slightly below the natural oscillation frequency. Thus, inertial design of the spacecraft would be constrained, but large roll angles could be maintained with small driving torques.

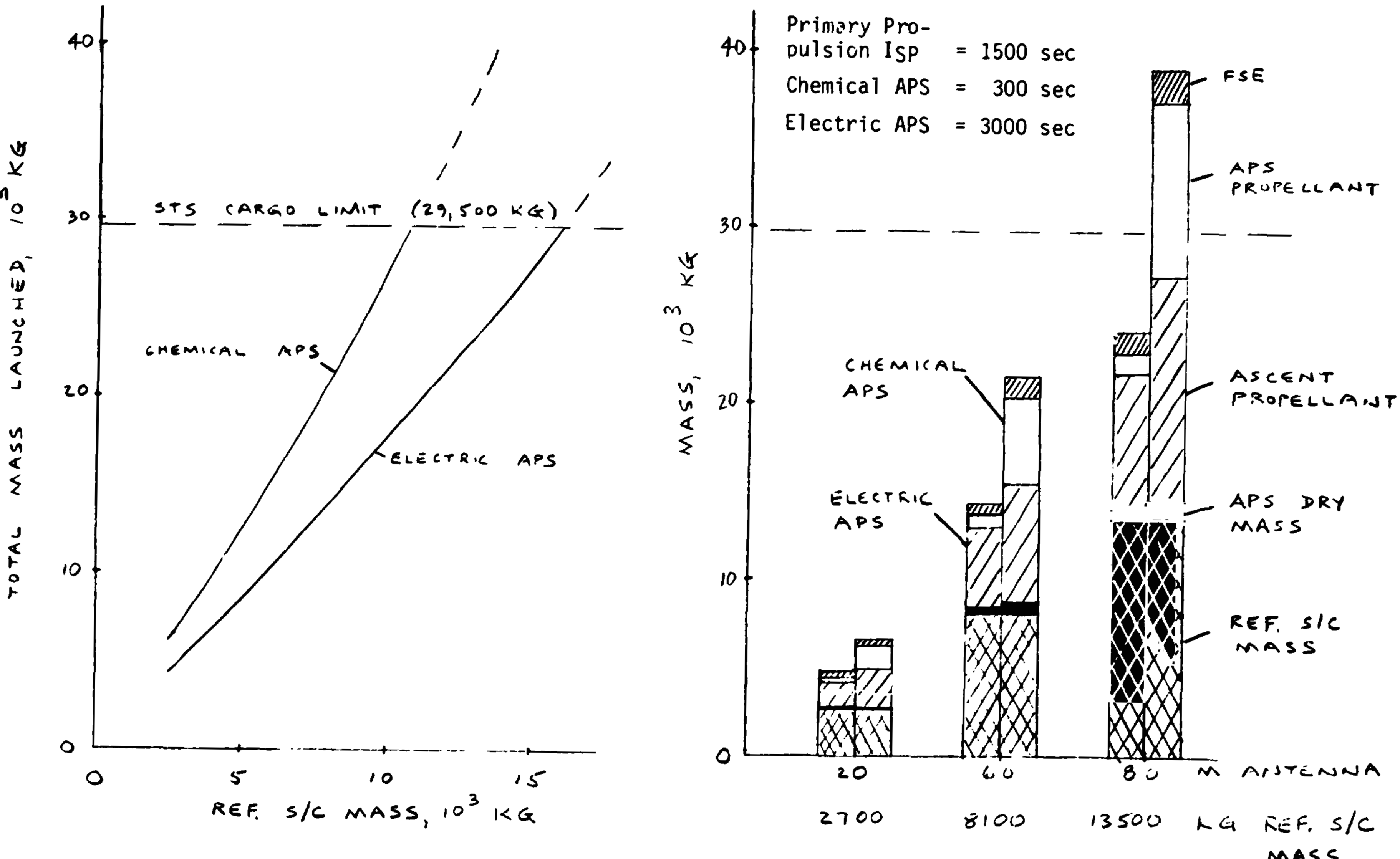

TOTAL MASS LAUNCHED

MASS BREAKDOWN

Figure 15. Performance Comparison of Chemical and Electric APS

Table 6. Spacecraft Attitude Maneuvers for Optimum Sun Alignment During Primary Thrust Phases

1. Lowest Altitude (ARRAY FEATHERED FOR MINIMUM DRAG)	Roll Only	Excursions ±38° for Sun Angle = 52° ±75° for Sun Angle = 15° Fixed 90° for Sun Angle ≤ 15°
2. Low-to-Intermediate Altitudes (ARRAY ARTICULATED)	Roll Only	SAME AS ABOVE
3. Intermediate-to-High Altitudes (ARRAY ARTICULATED; PLANE CHANGE SIMULTANEOUSLY WITH ORBIT RAISING)	Roll Yaw	Modified Periodic Exc[illegible]n Same Range Excursions to ±45° GENE[illegible]T IN PHASE WITH ROLL EXCURSIONS, DEPENDING ON NODAL POSITION RELATIVE TO SUN LINE

REFERENCES

1. C. H. Terwilliger and W. W. Smith, "Electric Propulsion for Near-Earth Space Missions," NASA CR-159736, NASA-LeRC Contract NAS 3-21346, January 1980.

2. W. W. Smith and J. P. Clark, "Study of Electrical and Chemical Propulsion for Auxiliary Propulsion of Large Space Systems," NASA CR-165502, NASA-LeRC Contract NAS 3-21952, March 1981.

3. W. E. Pipes, III, "Advanced Spacecraft Deployment System Study," AFRPL-TR-80-43, AFRPL Contract F04611-79-C-0032, September 1980.